Cell-surface protein YwfG of *Lactococcus lactis* binds to α-1,2-linked mannose

Short title: Lactococcal cell-surface protein binds to α-1,2-linked mannose

Wataru Tsuchiya[1], Zui Fujimoto[1], Noritoshi Inagaki[1], Hiroyuki Nakagawa[1], Miwa Tanaka[2], Hiromi Kimoto-Nira[3,#a], Toshimasa Yamazaki[1], Chise Suzuki[3,#b]*

[1] Research Center for Advanced Analysis, National Agriculture and Food Research Organization (NARO), Tsukuba, Ibaraki, Japan

[2] Asahi Quality & Innovations, Ltd, Moriya, Ibaraki, Japan

[3] Institute of Livestock and Grassland Science, NARO, Tsukuba, Ibaraki, Japan

[#a] Current Address: Institute of Food Research, NARO, Tsukuba, Ibaraki, Japan

[#b] Current Address: College of Bioresource Science, Nihon University, Fujisawa, Kanagawa, Japan

* Corresponding author

E-mail: suzuki.chise@nihon-u.ac.jp

Abstract

Lactococcus lactis strains are used as starter cultures in the production of fermented dairy and vegetable foods, but the species also occurs in other niches such as plant material. *Lactococcus lactis* subsp. *lactis* G50 (G50) is a plant-derived strain and potential candidate probiotics. Western blotting of cell-surface proteins using antibodies generated against whole G50 cells identified a 120-kDa protein. MALDI-TOF MS analysis identified it as YwfG, a Leu-Pro-any-Thr-Gly cell wall anchor domain–containing protein. Based on a predicted structure, a recombinant protein covering the N-terminal half (aa 28–511) of YwfG ($YwfG_{28–511}$) was crystallized and the crystal structure was determined. The structure consisted of an L-type lectin domain, a mucin-binding protein domain, and a mucus-binding protein repeat. Recombinant proteins containing combinations of these domains were prepared and their interactions with monosaccharides were examined by isothermal titration calorimetry; the only interaction observed was between the L-type lectin domain and D-mannose. Among four mannobioses, α1,2-mannobiose had the highest affinity for the L-type lectin domain (dissociation constant = 34 μM). The L-type lectin domain also interacted with yeast mannoproteins and yeast cells. Soaking of the crystals of $YwfG_{28–511}$ with mannose or α1,2-mannobiose revealed that both sugars bound to the L-type lectin domain in a similar manner, although the presence of the mucin-binding protein domain and the mucus-binding protein repeat within the recombinant protein inhibited the interaction between the L-type lectin domain and mannose. These findings provide new structural and functional insights into the interaction between *L. lactis* and its ecological niche via binding of the cell-surface protein YwfG with mannose.

Introduction

Gram-positive bacteria interact with their environment and other cells via proteins expressed on their cell surface. An important subset of these cell-surface proteins are the adhesins that mediate adhesion to other cells or environmental surfaces. For example, in the initial stages of colonization, pathogenic bacteria use their cell-surface proteins to bind to host cells [1].

In *Staphylococcus aureus*, mucus-binding proteins are anchored to the cell surface by a sortase A–mediated system that recognizes the motif LPXTG (Leu-Pro-any-Thr-Gly) [2]. In this system, the mucus-binding proteins are cleaved between the Thr and Gly of the LPXTG motif by sortase A and then undergo transpeptidation and covalent attachment to peptidoglycan in the bacterial cell wall. Sortase-anchored surface proteins fulfill key functions during the infectious process and thus sortase A is essential for host colonization and for the pathogenesis of invasive diseases. The roles of sortases and proteins containing the LPXTG motifs are well documented in pathogens, but even in nonpathogenic lactic acid bacteria a mechanism that mediates the relationship between cell surface proteins and the host that is analogous to that in pathogenic bacteria has been identified [3, 4].

Lactobacilli are Gram-positive bacteria in order *Lactobacillales*, strains of which are found in the human intestine and also used in the production of fermented foods. The strains that are used as probiotics are mostly of intestinal origin and are reported to adhere to the intestinal mucus layer [5]. Understanding the interaction between lactobacilli and mucins is critical to elucidate the survival strategies of lactobacilli in a constantly changing intestinal environment, as well as to elucidate the mechanisms of their beneficial effects in the intestinal tract. Cell-surface proteins likely play a key role in these strategies and mechanisms by interacting with host receptors, such as the glycans in mucins [3, 5]. Lactobacilli express several adhesins, including moonlighting proteins (multi-functional cytoplasmic proteins) that exert adhesive functions when expressed on the cell surface [6]. Several species of

68 Lactobacilli are known to possess surface-layers (S-layers) proteins [7] that are involved in
69 the adhesion of the cells to the host epithelium or to extracellular matrix components and in
70 the modulating the host immune response [3]. For example, knockout of the S-layer protein A
71 in *Lactobacillus acidophilus* significantly reduces binding of the mutant to DC-SIGN, a
72 dendritic cell (DC)–specific receptor, and the S-layer protein A is involved in the modulation
73 of DC and T-cell functions [8]. Whereas certain strains of lactobacilli bind to epithelial cells
74 via mucin in order to reside in the intestinal tract, other strains bind yeast cells used in
75 fermentation processes [9]. In some cases, symbiosis between the yeast and lactobacilli
76 improves fermentation [10, 11].

77 *Lactococcus* is another genus in order *Lactobacillales*. Strains belonging to *Lactococcus*
78 *lactis* and *Lactococcus cremoris* are used as fermentation starters in the production of cheese
79 and other dairy and vegetable fermented products. Originally, it was thought that lactococci
80 did not reach the intestinal tract alive, but Klijn et al. [12] showed that a fraction of viable
81 cells of a strain of *L. lactis* was able to survive passage through the human gastrointestinal
82 tract. Recently, several lactococcal strains have been reported to have beneficial health effects
83 such as improvement of skin status [13] and activation of human plasmacytoid DCs [14].
84 There are few studies on lactococcal surface proteins that interact with intestinal epithelium
85 or DCs

86 *Lactococcus lactis* is used extensively in the industrial production of fermented dairy
87 products. However, *L. lactis* strains have also been isolated from plant material [15, 16].
88 *Lactococcus lactis* subsp. *lactis* G50 (G50) was isolated from Napier grass and was
89 subsequently found to have immunostimulatory activity [17]. *In vitro*, intact G50, but not
90 heat-treated G50, can induce tumor necrosis factor α expression in the murine macrophage
91 cell line J774.1, suggesting that a heat-sensitive molecule is involved in this induction [18].
92 In ovomucoid-sensitized BALB/c mice, oral administration of intact G50 cells reduces total

93 IgE production [17]. Together, these findings indicate that G50 may have potential uses as a
94 probiotic.
95 Analysis of the G50 genome sequence [19] may help reveal the cell-surface proteins that
96 contribute to the activity of G50. Here, we detected a cell-surface protein by reaction of *L.*
97 *lactis* strains with anti-G50 antibody. We used matrix-assisted laser desorption/ionization–
98 time-of-flight mass spectrometry (MALDI-TOF MS) and X-ray crystallography to
99 investigate the structure and interactions of this protein.
100

101 Materials and Methods

102 Strains

103 Five lactococcal strains were used in this study (Table 1). The strains were grown at 30°C for
104 18 h in M17 (BD Difco, Sparks, MD, USA) broth containing 0.5% (wt/vol) glucose (GM17).
105 *Escherichia coli* BL21(DE3) (Merck, Darmstadt, Germany) was used for the expression of
106 recombinant proteins. Three yeast strains were also used: *Saccharomyces cerevisiae* X2180-
107 1A, *S. cerevisiae* AB9 [MAT a/α *gpi10/gpi10 ura3/URA3 leu2/LEU2*], and *S. cerevisiae*
108 AB9-2 [MAT a/α *gpi10/gpi10 mnn2/mnn2 ura3/URA3 leu2/LEU2*] [20]. YPD containing 1%
109 yeast extract, 2% peptone, and 2% glucose was used for culturing the yeast strains. A
110 synthetic defined medium (SD-medium) (yeast nitrogen base without amino acids containing
111 0.17% ammonium sulfate [BD Difco], 2% glucose, 0.13% casamino acids [BD Difco]) was
112 used for yeast culture for mannoprotein preparation.
113
114 **Table 1**. Lactococcal strains used in this study

Strain	Species	YwfG*	Origin
G50	*Lactococcus lactis* subsp. *lactis*	+	Napier grass [17]

S63	*L. lactis* subsp. *lactis*	-	Kimchi [18]
O29	*Lactococcus cremoris*	+	Kefir [15]
H46	*L. lactis* subsp. *lactis*	+	Kimchi [15]
H54	*L. lactis* subsp. *lactis*	+	Kimchi [15]
DRC1	*L. lactis* subsp. *lactis* bv. diacetylactis	+	NIRD [21]
N-7	*L. lactis* subsp. *lactis* bv. diacetylactis	+/-	Commercial cheese starter [21, 22]
CVT8W	*L. lactis* subsp. *lactis* bv. diacetylactis	+	Commercial cheese starter [23]
CVT3	*L. lactis* subsp. *lactis* bv. diacetylactis	+	Commercial cheese starter [23]
H59	*L. lactis* subsp. *lactis* bv. diacetylactis	+	Kimchi [15]
NIAI 527	*L. lactis* subsp. *lactis*	-	Laboratory collection [21, 22]
NIAI 712	*L. cremoris*	-	Laboratory collection [21, 22]
C13	*L. lactis* subsp. *lactis*	-	Cheese [15]
O31	*L. lactis* subsp. *lactis*	-	Kefir [15]
1256	*L. lactis* subsp. *lactis*	-	Raw milk [15]
S01	*L. lactis* subsp. *lactis*	-	Fermented milk [15]

*, The presence (+) or absence (-) of 120-kDa band corresponding to YwfG was examined by western blotting.

Preparation of cell-wall proteins

Five lactococcal strains showing high immunostimulatory activity in our previous study [18] were selected (Table 1). Cell-wall proteins were obtained by trypsin-mediated digestion of cell envelopes, as reported by Meyrand et al. [24]. Briefly, *L. lactis* cells were cultured to an optical density (OD_{600}) of 1.2 in 6 mL of GM17 medium at 30°C and centrifuged at 5000 × *g* for 10 min at 4°C. The cell pellet was washed once with 50 mM Tris-HCl (pH 7.0) and resuspended in 1 mL of 50 mM Tris-HCl (pH 7.0) containing protease inhibitors (cOmplete, Roche Applied Science, Mannheim, Germany). The cells were disrupted with glass beads using a FastPrep system (Qbiogene, Montreal, Quebec, Canada) set at 6.0 m s^{-1} for 40 s and

127 centrifuged at low speed (1000 × *g*) for 2 min at 4°C to remove the glass beads and any
128 unbroken bacteria. The supernatant was centrifuged at 16,000 × *g* for 15 min at 4°C. The
129 pellet containing the bacterial cell envelopes was digested with lysozyme (1 mg L^{-1}) and
130 mutanolysin (200 U mL^{-1}) in 50 mM Tris-HCl (pH 7.0) containing 5 mM $MgCl_2$ for 3 h at
131 37°C, centrifuged at 10,000 × *g* for 10 min at 4°C, and the supernatants were analyzed by
132 western blotting.
133

134 SDS-PAGE and western blotting

135 SDS-PAGE was performed in a 5%–20% linear gradient gel (Atto, Tokyo, Japan). Proteins
136 were visualized by Coomassie Brilliant Blue staining (CBB) or western blotting. After SDS-
137 PAGE, proteins were electrotransferred to a polyvinylidene difluoride membrane (Millipore,
138 Burlington, MA, USA) using a semi-dry transfer blotter (Atto). Rabbit polyclonal antiserum
139 to G50 was generated against intact G50 cells and purified by using a recombinant protein A
140 column (rProtein A Sepharose FF, Cytiva, Tokyo, Japan). The membrane was incubated with
141 anti-G50 antiserum (1:3000 dilution) and horseradish peroxidase–linked anti-rabbit
142 immunoglobulin (Bio-Rad Laboratories Inc., Hercules, CA, USA; 1:5000 dilution), and the
143 blot was developed with an ECL Prime western blotting kit (Cytiva).
144

145 Protein identification by MALDI-TOF MS and database
146 searching

147 CBB-stained bands corresponding to the bands detected by the anti-G50 antiserum were
148 excised from the gel and treated by in-gel digestion with a proteomics-grade trypsin (Sigma-
149 Aldrich, St Louis, MO, USA). The digested samples were purified by using ZipTip C18
150 (Merck). The purified peptides were mixed with an equal volume of α-cyano-4-

151 hydroxycinnamic acid (4-CHCA) (Shimadzu GLC Ltd., Tokyo, Japan) matrix solution
152 (prepared as 10 mg/mL in 50% acetonitrile containing 0.1% TFA), and an aliquot of the
153 mixture (0.5 μL) was spotted onto an ABI 4800 MALDI plate (SCIEX, Framingham, MA,
154 USA). The mass spectrometer, a MALDI-TOF/TOF mass spectrometer (4800 Plus TOF/TOF
155 analyzer, SCIEX) was tuned and calibrated using a calibration standards mixture (Peptide
156 Calibration Standard II, Bruker Daltonics GmbH & Co. KG, Bremen, Germany) prior to the
157 measurements. After the spot had been allowed to dry at room temperature, MS and MS/MS
158 spectra were obtained. Proteins were identified using a Mascot search engine (ver. 2.4.0.;
159 Matrix Science, London, UK) and the NCBI database.
160

161 **Protein sequence and structure analysis**

162 Protein sequence analysis and domain fold prediction were performed on the Pfam
163 (hhttps://pfam.xfam.org) and the Phyre2 (http://www.sbg.bio.ic.uk/phyre2) servers. Protein
164 structures were compared on the Dali server (http://ekhidna2.biocenter.helsinki.fi/dali/)[25].
165

166 **Preparation of YwfG variants**

167 Total bacterial DNA was isolated by using a DNeasy Blood & Tissue Kit (Qiagen, Hilden,
168 Germany). Primers were designed using the coding sequence (CDS) of locus tag
169 LLG50_11005 of the G50 genome sequence (accession number CP025500.1). The following
170 primers were used for the construction of four recombinant YwfG variants:
171

172 Fw28: 5′-CCGCGCGGCAGCCATATGCCCGACTCTTTTAAAATACAACGG-3′
173 Rv270: 5′-GAGCTCGAATTCGGATCCTCAACCTTGAGCTACCGTATAAGT-3′
174 Rv336: 5′-GAGCTCGAATTCGGATCCTCAATTTCGAGTATAAACATAGTT-3′
175 Rv511: 5′-GAGCTCGAATTCGGATCCTCAGTTACGTTTATAAACGACCTT-3′

176 Fw860: 5′-CCGCGCGGCAGCCATATGCAAGGAACCATTGATGTTACTTAT-3′

177 Rv1034: 5′-GAGCTCGAATTCGGATCCTCAAGGCACCTTATGATAAACGAC-3′

178

179 DNA fragments encoding variants of YwfG (residues 28–270, 28–336, 28–511, and 860–
180 1034) were amplified by polymerase chain reaction using the primer sets Fw28–Rv270,
181 Fw28–Rv336, Fw28–Rv511, and Fw860–Rv1034, respectively. The resulting fragments were
182 inserted in *Nde*I/*Bam*HI-digested pET28b (Merck) by In-Fusion cloning reactions (In-Fusion
183 HD Cloning Kit, Takara Bio, Kusatsu, Japan) with an N-terminal His_6-tag. The resulting
184 constructs were transformed into *E. coli* BL21(DE3). Recombinant YwfG variants were
185 expressed at 16°C overnight in the presence of 0.2 mM isopropyl β-D-thiogalactoside and
186 purified by affinity chromatography using a nickel-chelating column (HisTrap HP, Cytiva),
187 followed by gel filtration using a HiLoad 26/600 Superdex 75 pg column (Cytiva) and cation
188 exchange chromatography using a Mono S 10/100 GL column (Cytiva). The obtained
189 recombinant YwfG variants were named $YwfG_{28–270}$, $YwfG_{28–336}$, $YwfG_{28–511}$ (numbers
190 indicate amino acid residues), and MubR4 (residues 860–1034).

191

192 Preparation of yeast mannoproteins

193 *gpi10* mutants of *S. cerevisiae* secrete mannoproteins into the culture medium [20].
194 Mannoprotein of AB9 strain (wild-type) and of AB9-2 strain (*mnn2* mutant lacking α1,2-
195 mannosyltransferase) were prepared. Yeast cells were cultured in the SD-medium for 6 days
196 at 30°C. The cultures were centrifuged at 12,000 ×*g* for 10 min at 4°C to obtain a cell-free
197 supernatant. The mannoproteins were concentrated using a 10,000 molecular-weight-cut-off
198 ultrafiltration unit (Centriprep, Merk Millipore, Cork, Ireland), precipitated by adding 2
199 volumes of ethanol, and dissolved in 20 mM Tris-HCl (pH 7.5).

200

201 # Isothermal titration calorimetry (ITC) analysis

202 A MicroCal iTC200 system (Malvern Panalytical, Almelo, Netherlands) was used to measure
203 enthalpy changes associated with interactions between the YwfG variants and the following
204 yeast cell-wall components: the monosaccharides D-glucose, D-galactose, D-mannose, D-
205 fucose, *N*-acetyl-D-glucosamine (GlcNAc), and 2-(acetylamino)-2-deoxy-D-galactose
206 (GalNAc) (Sigma-Aldrich); α1,2-, α1,3-, α1,4-, and α1,6-mannobiose (Dextra Laboratories,
207 Reading, UK); mannan from *S. cerevisiae* (Sigma-Aldrich); and yeast mannoproteins.

208 A solution of YwfG variant (100 μM $YwfG_{28–270}$, $YwfG_{28–336}$, $YwfG_{28–511}$, or MubR4 in
209 20 mM Tris-HCl [pH 7.5]) was placed in a 200-μL calorimeter cell, and test solution (10 mM
210 for monosaccharides, 2 mM for monosaccharides and mannobioses, 10 mg mL^{-1} for yeast
211 mannan, OD_{280} 1.0 for mannoproteins) was loaded into the injection syringe. The test
212 solution was titrated into the sample cell as a sequence of 20 injections of 2-μL aliquots each.
213 All experiments were performed at 25°C.

214

215 # Crystallization, data collection, and structure refinement

216 Purified $YwfG_{28–511}$ was concentrated to 12.0 mg mL^{-1} and crystallized by the sitting-drop
217 vapor diffusion method at 20°C using a precipitant solution consisting of 0.1 M sodium
218 acetate (pH 5.0–5.6), 1.3 M Li_2SO_4, and 2% (w/v) polyethylene glycol 3350 (Hampton
219 Research, Aliso Viejo, CA, USA). We used 50 μL of the reservoir solution and a drop
220 consisting of 0.5 μL of the protein solution and 0.5 μL of the reservoir solution; plate-type
221 crystals appeared within 2–3 weeks.

222 Diffraction data were collected at two beamlines: BL-5A housed at the Photon Factory
223 and BL-NW12 housed at the Photon Factory Advanced Ring (both at the High Energy
224 Accelerator Research Organization, Tsukuba, Japan). Diffraction data were collected using a

225 Pilatus3 S6M or Pilatus3 S2M detector (Dectris, Philadelphia, PA, USA). Crystals were
226 collected in a 0.5-mm nylon cryoloop (0.5 mm, Hampton Research), soaked in a precipitant
227 drop containing 30% (v/v) glycerol, and cryocooled in a nitrogen gas stream to 95 K. Crystals
228 in complex with D-mannose or α1,2-mannobiose were obtained by adding 0.5 μL 10% D-
229 mannose or α1,2-mannobiose solution to the crystal drop a few minutes prior to the
230 diffraction experiment. The data were integrated using the XDS program package [26] and
231 scaled using the SCALA program [27] within the CCP4 program suite [28].
232 The ligand-free structure of $YwfG_{28–511}$ was determined by the molecular replacement
233 method using the Molrep program [29] with the lectin domain (residues 258–492) of SraP
234 (PDB code 4m01 [30]) as the search model. Sugar complex structures were built using the
235 ligand-free structure as the starting model. Manual model building and molecular refinement
236 were performed using Coot [31] and Refmac5 [32]. Data collection and refinement statistics
237 are shown in Table 2. The stereochemistry of the models was analyzed using the MolProbity
238 program [33] and structural drawings were prepared using the PyMOL
239 (https://www.pymol.org/pymol.html) or Cuemol2 program (http://cuemol.osdn.jp/en/).
240
241 **Table 2.** Data collection and refinement statistics of the YwfG fragment structures

	Native	D-mannose complex	α1,2-mannobiose complex
PDB code	7YL4	7YL5	7YL6
Data collection			
Space group	*I*222	*I*222	*I*222
Cell parameters (Å)	*a* = 43.2	*a* = 43.3	*a* = 43.5
	b = 272.9	*b* = 273.2	*b* = 276.6
	c = 320.3	*c* = 322.8	*c* = 321.8
X-ray source	PF-AR BL-NW12	PF BL-5A	PF-AR BL-NW12
Wavelength (Å)	1.00000	1.00000	1.00000

Resolution (Å)	48.6–2.50 (2.64–2.50)	48.7–3.00 (3.16–3.00)	43.06–2.95 (3.11–2.95)
No. of reflections	871 880 (127 582)	507 098 (73 143)	546 645 (84 290)
Unique reflections	66 894 (9 601)	39 549 (5 675)	42 029 (6 070)
Completeness (%)	100.0 (100.0)	100.0 (100.0)	99.9 (100.0)
Multiplicity	13.0 (13.3)	12.8 (12.9)	13.0 (13.9)
R-merge	0.093 (0.810)	0.145 (1.053)	0.203 (1.187)
Average I/σ	21.3 (3.4)	16.0 (2.7)	14.0 (2.5)
Refinement			
Resolution (Å)	45.5–2.50 (2.57–2.50)	45.6–3.00 (3.08–3.00)	41.5–2.95 (3.03–2.95)
R-factor	0.246 (0.385)	0.227 (0.365)	0.211 (0.361)
R-free	0.280 (0.395)	0.296 (0.392)	0.268 (0.387)
No. of water molecules	74	33	41
Average *B*-value ($Å^2$)	65.1	79.9	65.2
r.m.s.d. from ideals			
lengths (Å)	0.011	0.021	0.014
angles (°)	1.75	2.28	2.03
Ramachandran plot (%) (favored/allowed/disallowed)	94.7 / 5.0 / 0.3	93.7 / 5.5 / 0.8	95.4 / 4.3 / 0.3

*Values in parentheses refer to the highest-resolution shell. r.m.s.d., root-mean-square deviation.

Interaction of yeast cells and YwfG variants

Saccharomyces cerevisiae X2180-1A was cultured in YPD medium to an OD_{600} of 0.6. In microplate wells, 50 μL yeast culture, 10 μL each recombinant YwfG protein (10 μM), and 40 μL PBS or each mannobiose (10 mM) were mixed and left to settle for 1–2 h, after which aggregation was observed.

Results

Identification of cell-surface proteins that reacted with anti-G50 antibody

Cell-surface proteins from five lactococcal strains (G50, S63, O29, H46, and H54) were prepared and analyzed by western blotting using an antibody generated against live G50 cells (Fig 1). A 37-kDa band was detected in all strains, and a strong 120-kDa band was detected in G50, O29, H46, and H54, but not in S63. Among 11 additional lactococcal strains examined (Table 1), the 120-kDa band was detected in 5 strains (data not shown), suggesting that this protein is not ubiquitous. The CBB-stained 120-kDa and 37-kDa bands were excised, subjected to in-gel trypsin digestion, and analyzed by MALDI-TOF MS and a Mascot search. The obtained peptide fragments from the 120-kDa protein were all aligned to the translated sequence of a CDS（LLG50_11005, GenBank: AUS70730.2) of the G50 genome (Fig 2). This protein consists of 1107 residues and contains mucus-binding protein repeats and the LPXTG motif. The peptide fragments from the 120-kDa protein from strains O29, H46, and H54 were almost the same as those from strain G50. Interestingly, a C-terminal peptide sequence DSKPTDVLPSTGDSQK containing LPSTG was detected in the 120-kDa proteins of strains G50, O29, H46, and H54, suggesting that this LPXTG-motif is not used for anchoring the protein to the cell wall.

Fig 1. Western blot and Coomassie Brilliant Blue staining of lactococcal cell-surface proteins. (A) Western blot of cell-surface proteins of five Lactococcal strains using anti-G50 antibody. (B) Coomassie Brilliant Blue staining of the same samples. The black triangle indicates the thin band of the 120-kDa protein.

275 **Fig 2. Deduced amino acid sequence of LLG50_11005 and peptides obtained by MALDI-**
276 **TOF MS analysis.** Peptides obtained were aligned to the deduced sequence and are shown
277 underlined and in bold. Peptides that were detected on both sides of the trypsin cleavage site
278 are indicated by a triangle.
279
280 Amino acid sequence analysis using the Phyre2 (http://www.sbg.bio.ic.ac.uk/phyre2) and
281 Pfam program (http://pfam.xfam.org/) indicated that the 120-kDa protein contained a
282 leguminous-type (L-type) lectin domain (Lec), a mucin-binding protein domain (Mbp), and
283 four mucus-binding protein repeats (MubRs), followed by a C-terminal LPXTG motif (Fig
284 3). From its similarity to the LPXTG cell-wall-anchor-domain–containing protein of *L. lactis*
285 subsp. *lactis* Il1403 (GenBank: AYV53882.1) [34], we named the protein YwfG, although
286 the N-terminal 180 amino acid residues of YwfG of G50, including the lectin domain, are
287 missing from that of Il1403.
288
289 **Fig 3. Schematic drawing of YwfG and constructions of variants.** (Top) Predicted domain
290 organization of YwfG. (Bottom) Recombinant variants constructed in the present study.
291
292 A Mascot search suggested that the 37-kDa protein was a phosphoglycerate kinase
293 (GenBank: AUS68744.1). Because phosphoglycerate kinases have been reported to be cell-
294 surface adhesins in *Ligilactobacillus agilis* [35] and Streptococci [36], the present lactococcal
295 phosphoglycerate kinase could possibly function as a moonlighting protein on the cell
296 surface.
297

298 # Interactions of the YwfG variants with monosaccharides and
299 mannobioses

300 Four recombinant YwfG variants ($YwfG_{28–270}$, Lec domain; $YwfG_{28–336}$, Lec and Mbp;
301 $YwfG_{28–511}$, Lec, Mbp, and MubR1; and MubR4) were expressed and purified (Fig 3).
302 Glycoconjugate microarray analysis revealed that $YwfG_{28–270}$ did not bind to human-type
303 glycan (data not shown). The binding of the four variants with six monosaccharides (D-
304 glucose, D-galactose, D-mannose, D-fucose, GlcNAc, and GalNAc) was examined using ITC.
305 The only combination of variant and monosaccharide that showed an interaction was
306 $YwfG_{28–270}$ with D-mannose; that is, the Lec domain alone could bind to D-mannose.
307 The binding of the three variants to four mannobioses (α1,2-, α1,3-, α1,4-, and α1,6-
308 mannobiose) was also examined using ITC. The thermodynamic parameters for the
309 interactions observed in the ITC assay are shown in Table 3. No binding of $YwfG_{28–336}$, or
310 $YwfG_{28–511}$ to any mannobiose was observed. $YwfG_{28–270}$ bound to all of the mannobioses,
311 but the binding capacity of α1,2-mannobiose was the greatest; the dissociation constant of
312 α1,2-mannobiose (K_D = 34 μM) was much lower than that of D-mannose (K_D = 500 μM).
313

314 **Table 3.** Thermodynamic parameters from isothermal titration calorimetry assay

Substrate	N (sites)	K_D (μM)	ΔH (cal/mol)	ΔS (cal/mol/deg)
D-mannose*	(1.00)	500 ± 37	−2098 ± 83.59	8.07
α1,2-mannobiose	1.19 ± 0.0104	34.4 ± 0.97	−5236 ± 62.07	2.86
α1,3-mannobiose	0.757 ± 0.148	172 ± 21	−6073 ± 1387	−3.15
α1,4-mannobiose	1.82 ± 0.171	328 ± 91	−2206 ± 309.7	9.55
α1,6-mannobiose	1.21 ± 0.0839	210 ± 13	−4235 ± 372.8	2.62

315 * Thermodynamic parameters determined with fixed stoichiometry (N = 1).
316 N, stoichiometry; K_D, dissociation constant; ΔH, enthalpy change; ΔS, entropy change.

317

318 ## Crystal structure of $YwfG_{28–511}$

319 Next, we elucidated the crystal structure of recombinant $YwfG_{28–511}$. We solved it by the
320 molecular replacement method at 2.50-Å resolution (Table 2). The crystal belonged to space
321 group *I*222 with two molecules (I and II) per asymmetric unit. Molecule I was modeled with
322 continuous residues from 40–511, whereas only residues 41–417 and 446–465 were modeled
323 in molecule II. The electron density map of N-terminal residues 28–39 could not be modeled
324 in either molecule. $YwfG_{28–511}$ fragment had an overall elongated shape with an overall
325 diameter of 40 Å and length of 180 Å, comprised 35 β-sheets and 4 α-helices, and was
326 formed by head-to-tail tandem connection of the three domains, Lec, Mbp, and MubR1 (Fig
327 4A, B). Compared with molecule I, molecule II had a more bent structure with a larger angle
328 between domains (Fig 4C).

329

330 **Fig 4. Overall structure of $YwfG_{28–511}$.** (A) X-ray crystal structure and (B) topology diagram
331 of $YwfG_{28–511}$ molecule I. The Lec, Mbp, Sub-N, Sub-C domains, and calcium ion are colored
332 blue, green, orange, red, and black, respectively. (C) Superimposition of the crystal structures
333 of $YwfG_{28–511}$ molecules I (green) and II (red).

334

335 Starting from the N-terminus, the first domain (residues 41–268) had a jelly roll–type β-
336 sandwich structure comprising 15 β-strands and 3 short α-helices. The core structure
337 consisted of an antiparallel β-sheet fold formed from two sheets: sheet-I (β1, β3, β5, β10-12,
338 β14, and β15) and sheet-II (β2, β4, β6-β9, and β13). A calcium-binding site was observed
339 between sheet-II and the loop connecting the β7 and β8 strands (loop 7–8). One Ca^{2+} ion was
340 coordinated by Asp152 (Oδ1 and Oδ2) belonging to β7; Tyr154 (O), Asn156 (Oδ1), and
341 Asp166 (Oδ1) located in loop 7–8; and one water molecule. Structural similarity analysis

342 using the Dali server [25] revealed that this domain had the highest similarity to *S. aureus*
343 SraP lectin domain (PDB code 4m01), with a structural alignment Z-score of 35.5 and root-
344 mean-square deviation (r.m.s.d). of 1.4 Å over 226 aligned residues (Fig 5A).
345
346 **Fig 5. Comparison of YwfG domain structures. (**A) Superimposed ribbon models of the Lec
347 domain of YwfG (green) and *Staphylococcus aureus* SraP (light blue, PDB code 4m01). (B)
348 Superimposition of the Mbp domain structures of YwfG (green) and *L. monocytogenes*
349 Imo0835 (yellow, PDB code 2kvz; pink, PDB code 2kt7). Superimposition of the (C) Sub-N
350 and (D) Sub-C structures of YwfG MubR1 on the B1 and B2 subdomains, respectively, of *L.*
351 *reuteri* MubRV (cyan, PDB code 4mt5) and MubR5 (magenta, PDB code 3i57).
352
353 The second domain (residues 271–336) comprised six β-strands folded in a β-sandwich
354 composed of a mixed β-sheet formed from β16, β17, β19, and β21 and an antiparallel β-sheet
355 consisting of β18 and β20. This structure is similar to the Mbp domains of *Listeria*
356 *monocytogenes* mucin-binding and putative peptidoglycan-binding protein Imo0835 (PDB
357 codes 2kt7 and 2kvz, respectively) with a structural alignment Z-score of 7.7–8.2 and r.m.s.d.
358 of 1.6–1.9 Å over 64–66 Cα atoms (Fig 5B).
359 The third domain (residues 337–511) had a structure in which two subdomains were
360 connected by a three-stranded β-sheet. The N-terminal subdomain (Sub-N, residues 337–409)
361 had a structure called a ubiquitin-like β-grasp fold, similar to that found in proteins in the
362 immunoglobulin-binding superfamily, formed from six β-strands (β22–β27) and one α-helix
363 (α4). The C-terminal subdomain (Sub-C, residues 410–511) consisted of a second domain-
364 like fold formed from six β-strands (β28, β29, β32–β35) and a twisted antiparallel β-sheet
365 (β28, β30, β31) located between the subdomains. The modeling of Sub-C in molecule (II)
366 was incomplete because the electron density map was unclear. Structural comparison analysis

367 revealed that the third YwfG domain showed high similarity with MubR folds of a mucus-
368 binding protein from *Limosilactobacillus reuteri*, Mub-RV (PDB code 4mt5) [4] and Mub-R5
369 (PDB code 3i57) [37], with a Z-score of 12.3–14.5 and r.m.s.d. of 3.3–6.3 Å over 155–165
370 aligned residues. The Sub-N and Sub-C domains of YwfG were very similar to the B1 and
371 B2 domains of the *L. reuteri* MubRs, respectively, although the β-sheet of the third domain of
372 YwfG is more bent (Figure 5C, D).
373

374 **Substrate recognition mechanism**

375 A structural analysis of the substrate-binding complex was performed to elucidate the
376 substrate recognition mechanism of YwfG for the glycoconjugates with which an interaction
377 was confirmed by the ITC assay. To obtain crystals of substrate-bound YwfG, ligand-free
378 crystals were soaked in a solution containing D-mannose or α1,2-mannobiose. The structures
379 of the D-mannose– and α1,2-mannobiose–YwfG$_{28–511}$ complexes were determined at 3.00 Å
380 and 2.95 Å, respectively. In each complex, a single substrate molecule was bound to the
381 recognition site, which was located in the groove-like region between loop 7–8 and loop 13–
382 14 on the YwfG$_{28–270}$ surface and partially overlapped with the calcium-binding site.
383 In the Man–YwfG$_{28–511}$ complex, the recognition of D-mannose by the Lec domain was
384 the result of a hydrogen bond network involving six amino acid residues (Fig 6A). The D-
385 mannose-OH6 group was recognized by the main-chain N of Gly250 and Phe252 and the
386 main-chain O of Phe252 in loop 13–14. The main-chain amide of Ala251 also formed a
387 hydrogen bond with D-mannose-O5. The D-mannose-OH4 group interacted with the
388 sidechain of Asn156 (Nδ2) coordinating with the calcium ion and sidechain of Asp117 (Oδ1)
389 in the β6 strand. Furthermore, the D-mannose-OH3 group interacted indirectly with the main-
390 chain N of Gly136 in loop 6–7 via a water molecule. In addition, the aromatic sidechain of
391 Tyr154 formed a CH-π stacking interaction with the hydrophobic face of D-mannose.

392

393 **Fig 6. Substrate recognition by the YwfG Lec domain.** (A) D-mannose and (B) α1,2-
394 mannobiose binding mechanism. The sugar substrate molecules and the YwfG residues that
395 interact with these are indicated by the yellow and green ball-and-stick models, respectively.
396 Calcium ions are shown as blue-white spheres.

397

398 The crystal structure of the α1,2-mannobiose–$YwfG_{28–511}$ complex showed a wider range
399 of substrate interactions than was seen for the recognition of mannose (Fig 6B). The OH4
400 group of the non-reducing terminal mannose residue (mannose-1) formed a hydrogen bond
401 with the sidechain of the Ser81 (Oγ) in loop 3–4. The reducing terminal mannose residue
402 (mannose-2) was recognized in a manner similar to that of the monosaccharide mannose. The
403 mannose-2-OH1 group was not involved in the recognition mechanism and was oriented
404 toward the open space outside the ligand-binding pocket.

405

406 Interaction of YwfG domains with yeast mannoproteins

407 Yeast *gpi10* mutants secrete mannoproteins into the culture media [20]. Here, secreted
408 mannoproteins were concentrated from the culture filtrate by ultrafiltration and ethanol
409 precipitation. Interaction of $YwfG_{28–270}$ with mannoproteins was examined using ITC.
410 Thermal energetic changes, which indicate an interaction, were observed for mannoproteins
411 obtained from AB9 and AB9-2 and for the commercial yeast mannan. Yeast mannoproteins
412 are highly glycosylated cell-wall proteins consisting of 20% protein and 80% D-mannose.
413 Mannoprotein from AB9 is wild-type high-mannose glycan, whereas that from AB9-2 is
414 high-mannose glycan lacking α1,2-linked mannose. Consistent with the observed binding
415 capacity to α1,2-mannobiose (Table 2), the interactions of $YwfG_{28–270}$ with mannoprotein

416 from AB9 and yeast mannan were more intense than that with the mannoprotein from AB9-2
417 (Fig 7).
418
419 **Fig 7. Interaction of $YwfG_{28–270}$ with yeast mannan proteins.** Isothermal titration of
420 $YwfG_{28–270}$ against (A) AB9 (wild type), (B) AB9-2 (mnm2 mutant) mannoprotein, (C) SD-
421 medium, and (D) yeast mannan.
422

423 # Interaction of YwfG domains with yeast cells

424 The interactions of the four recombinant domains ($YwfG_{28–270}$, $YwfG_{28–336}$, $YwfG_{28–511}$, and
425 MubR4) with yeast X2180-1A, which expresses high-mannose glycans on its cell surface,
426 were investigated (Fig 8). When yeast X2180-1A and 1 μM of each recombinant protein were
427 added to the well of a round-bottomed titer plate, cells were distributed uniformly at the
428 bottom of the wells in the presence of $YwfG_{28–270}$, $YwfG_{28–336}$, $YwfG_{28–511}$, but not in the
429 presence of MubR4 (Figure 8A). Such a uniform distribution is observed in yeasts that
430 aggregate [38]. The aggregation induced by $YwfG_{28–336}$ and $YwfG_{28–511}$ but not by $YwfG_{28–}$
431 $_{270}$ was inhibited by the addition of 1 mM D-mannose (data not shown). Similarly, when 1
432 mM mannobiose was added, the aggregation induced by $YwfG_{28–336}$ and $YwfG_{28–511}$ but not
433 by $YwfG_{28–270}$ was inhibited in the presence of α1,2- or α1,3-mannobiose (Fig 8B).
434
435 **Fig 8. Interaction of YwfG variants with yeast cells and mannobioses.** (A) Yeast cells in
436 the presence (+) or absence (−) of 1 μM of each variants (270 [$YwfG_{28–270}$], 366 [$YwfG_{28–366}$],
437 511 [$YwfG_{28–511}$], MR [MubR4]). (B) Yeast cells in the presence of 1 μM of each variant and
438 1 mM each mannobiose (α1,2, α1,3, α1,4, α1,6-mannobiose).
439

440 # Discussion

441 Here, we found that YwfG is a cell-surface protein that reacts with a strain-specific antibody
442 against *L. lactis* G50. This protein was presumed to be covalently bound to the cell wall via
443 the LPXTG motif by sortase, but we found no evidence of cleavage at the motif or binding of
444 the protein to the cell wall. Cleavage by sortase occurs between the Thr and Gly of the
445 LPXTG motif. If YwfG is covalently attached to the cell wall by the sortase, the C-terminal
446 amino acid sequence after the Thr residue should not be detected. However, a peptide
447 sequence including LPSTG (DSKPTDVLPSTGDSQK) was detected by MALDI-TOF MS
448 not only in YwfG of strain G50 but also in that of the other strains examined, indicating that
449 at least part of YwfG is present on the cell surface without being anchored to the cell wall.

450 Structural analysis revealed that $YwfG_{28–511}$ is composed of three different domains: Lec,
451 Mbp, and MubR. These domains have structural features of many gram-positive bacterial cell
452 wall adhesins, suggesting that YwfG has a similar function [4, 37, 39, 40]. Adhesins are
453 considered to function most effectively when their substrate-binding sites protrude as far as
454 possible from the bacterial surface [4]. *Lactococcus lactis* G50 YwfG has a Lec domain at the
455 tip of an approximately 600–650-Å long column consisting of one Mbp and four MubRs
456 extending from the cell wall, suggesting that the structure is suitable for binding to distant
457 target glycans.

458 The Lec domains of YwfG and *S. aureus* SraP have similar structures, although their
459 substrate specificities differ markedly. The legume (L)-type lectin–like module of SraP
460 specifically binds to *N*-acetylneuraminic acid and may mediate adhesion of *S. aureus* to host
461 sialylated receptors and interaction of *S. aureus* with host epithelial cells [30]. In contrast, the
462 ITC analysis in the present study revealed that $YwfG_{28–270}$ exhibits high affinity for D-
463 mannose and mannobiose, especially α1,2-mannobiose. Crystallographic analysis of the
464 YwfG–substrate complexes provided structural evidence of this substrate specificity. In the

465 recognition mechanism of α1,2-mannobiose by YwfG, mannose-2 (the reducing terminal
466 mannose residue) was involved in multiple interactions, whereas only one hydrogen bond
467 was observed for mannose-1 (the non-reducing terminal mannose residue), indicating that
468 mannose-2 and mannose-1 are the major and auxiliary recognition sites, respectively.
469 Furthermore, the mannose-2-OH1 group is not involved in the interaction and is oriented
470 toward the outside of the substrate-binding pocket. Since the OH1 group contributes to the
471 polymerization of sugars, we hypothesize that the Lec domain of YwfG will also bind to
472 longer-chain sugars possessing the mannose-α1,2- mannose structure. This difference in the
473 sugar-binding affinities of the Lec domains of lactococcal YwfG and the L-type lectin-like
474 modules of staphylococcal SraP may explain the different host specificities, with the former
475 interacting with plant substrates or yeast cells and the latter interacting with intestinal
476 epithelium.

477 Because YwfG was recognized by an anti-G50 antibody that was raised against intact
478 G50 cells, YwfG was recognized as epitopes and should interact with host immune cells. *L.*
479 *reuteri* mucus-binding protein repeats, Mub-R5 and Mub-RV, which have high structural
480 similarity to the MubR domain of YwfG, have been reported to bind not only to mucin
481 glycans but also to mammalian secretory Ig such as IgA, IgM, and IgG at the mucosal surface
482 of the digestive tract [37]. These interactions of the *L. reuteri* MubRs are considered to
483 contribute to the promotion of bacterial retention in the host mucosal epithelium and the
484 modulation of host immune responses [37]; MubR of YwfG may have similar functions.
485 Mannose-specific adhesin (Msa) of *Lactiplantibacillus plantarum* WCSF-1 also contains a
486 MubR and an L-type lectin domain, as does YwfG, and its mannose-specific binding function
487 is considered an essential factor for the probiotic properties of *L. plantarum* WCSF-1 [39].
488 The lectin domains of Msa and YwfG, which contribute to mannose-specific binding, have
489 only 37% amino acid identity. Mannose binding may be necessary for *L. lactis* to bind to

490 plant substrates or yeast cells. Similarly, it may play an important role in interactions with
491 mannose-containing receptors and other factors in the gastrointestinal tract. Further studies
492 are required to elucidate the role of *L. lactis* YwfG in the host–probiotic interaction and the
493 host response when bacterial adhesins adhere to intestinal epithelial cells or immune cells.
494 Blastp search [41] showed that at least 55 lactococcal strains have YwfG homologs with
495 more that 90% identity and query cover. YwfG occurs with or without an N-terminal Lec
496 domain and with various numbers of MubRs. The plant-derived *L. lactis* KF147 has a CDS of
497 YwfG (GenBank: ADA65975.1) with complete Lec, Mbp, and two MubR domains.
498 *Lactococcus cremoris* MG1363, a plasmid-free progeny of the dairy starter strain NCDO712,
499 has a CDS of YwfG (GenBank: CAL99029.1) with complete Lec, Mbp, and three MubR
500 domains. The complete set of amino acid residues involved in mannose and calcium binding
501 (D117, D152, D166, N156, Y154, and A251) are conserved in the Lec domains of YwfG of
502 strains KF147, MG1363, and G50. In contrast, *L. lactis* Il1403 has a CDS of YwfG
503 (GenBank: AYV53882.1) lacking half (120 amino acid residues) of the N-terminal Lec
504 domain of YwfG, suggesting that this protein does not bind mannose residues. The YwfG of
505 Il1403 has been confirmed to be a cell-wall-associated protein that is present in the wild-type
506 strain and absent in the sortase A mutant [34], suggesting that those proteins are likely
507 substrates of sortase A. Since this previous study did not report peptide sequences obtained
508 by MALDI-TOF MS, it is unknown whether the LPXTG motif of IL1403 is cleaved and used
509 for binding to the cell wall.
510 Strains of *L. lactis* are widely used in the production of fermented vegetables and various
511 fermented dairy products, and these strains are frequently isolated from non-dairy niches,
512 including soil and plant substrates [42]. The plant-derived *L. lactis* KF147 has gene sets for
513 degrading complex plant polymers and is adapted to grow on substrates derived from plant
514 cell walls [43]. Some plant cell walls contain galactomannans and glucomannans, which are

515 polymers consisting primarily of mannose (α-D-mannosides). Degradation of mannans to D-
516 mannose can be followed by conversion to D-fructose by mannose isomerase. In the present
517 study, a 35-kb region (1462553 to 1497747) of the G50 genome showed more than 98%
518 identity with 100% coverage with more than 40 *Lactococcus* strains including KF147 and
519 Il1403. This region encodes various proteins involved in glycan degradation and transport,
520 such as fructokinase, β-glucosidase, endo-β-*N*-acetylglucosaminidase, glucohydrolase, lacto-
521 *N*-biosidase, sugar transporters, α-mannosidases, and xylose operon. These proteins therefore
522 may contribute to the degradation of mannans and/or plant substrates and uptake of
523 monosaccharides for the growth of the strains Anchoring lectins that bind to mannose-
524 containing glycans distributed in plant cell walls to the cell-surface layer may be a necessary
525 strategy for degrading plant substrates.
526 Here, we experimentally clarified the structure and function of the lactococcal cell surface
527 protein YwfG. Categorized as a mucus-binding protein, this protein is homologous to the
528 *Staphylococcus aureus* SraP lectin, but unlike the lectins of the pathogenic bacteria, YwfG
529 bound mannose. These findings provide new structural and functional insights into the
530 interaction between *L. lactis* and its ecological niche, showing that these interactions are
531 distinct from the bacteria–host interactions of pathogenic bacteria.
532

533 # Acknowledgements

534 This work was supported in part by JSPS KAKENHI grant number 17K07741 (to C. S.).
535 The authors thank Ms. Tomoko Sato for her outstanding technical support in the MALDI-
536 TOF MS analysis.
537

538 # References

539 1. Chan JM, Gori A, Nobbs AH, Heyderman RS. Streptococcal serine-rich repeat proteins in
540 colonization and disease. Front Microbiol. 2020;11:593356. doi: 10.3389/fmicb.2020.593356.
541 2. Schneewind O, Missiakas D. Sortases, surface proteins, and their roles in *Staphylococcus aureus*
542 disease and vaccine development. Microbiol Spectr. 2019;7(1). doi: 10.1128/microbiolspec.PSIB-0004-2018.
543 3. Muscariello L, De Siena B, Marasco R. *Lactobacillus* cell surface proteins involved in interaction
544 with mucus and extracellular matrix components. Curr Microbiol. 2020;77(12):3831-3841. doi:
545 10.1007/s00284-020-02243-5.
546 4. Etzold S, Kober OI, Mackenzie DA, Tailford LE, Gunning AP, Walshaw J, et al. Structural basis for
547 adaptation of lactobacilli to gastrointestinal mucus. Environ Microbiol. 2014;16(3):888-903. doi: 10.1111/1462-
548 2920.12377.
549 5. Nishiyama K, Sugiyama M, Mukai T. Adhesion properties of lactic acid bacteria on intestinal mucin.
550 Microorganisms. 2016;4(3). doi: 10.3390/microorganisms4030034.
551 6. Savijoki K, Nyman TA, Kainulainen V, Miettinen I, Siljamäki P, Fallarero A, et al. Growth mode and
552 carbon source Impact the surfaceome dynamics of *Lactobacillus rhamnosus* GG. Front Microbiol.
553 2019;10:1272. doi: 10.3389/fmicb.2019.01272.
554 7. Hynönen U, Palva A. Lactobacillus surface layer proteins: structure, function and applications. Appl
555 Microbiol Biotechnol. 2013;97(12):5225-5243. doi: 10.1007/s00253-013-4962-2.
556 8. Konstantinov SR, Smidt H, de Vos WM, Bruijns SC, Singh SK, Valence F, et al. S layer protein A of
557 Lactobacillus acidophilus NCFM regulates immature dendritic cell and T cell functions. Proc Natl Acad Sci U S
558 A. 2008;105(49):19474-19479. doi: 10.1073/pnas.0810305105.
559 9. Yamasaki-Yashiki S, Sawada H, Kino-Oka M, Katakura Y. Analysis of gene expression profiles of
560 *Lactobacillus paracasei* induced by direct contact with *Saccharomyces cerevisiae* through recognition of yeast
561 mannan. Biosci Microbiota Food Health. 2017;36(1):17-25. doi: 10.12938/bmfh.BMFH-2016-015.
562 10. Hirayama S, Furukawa S, Ogihara H, Morinaga Y. Yeast mannan structure necessary for co-
563 aggregation with Lactobacillus plantarum ML11-11. Biochem Biophys Res Commun. 2012;419(4):652-655.
564 doi: 10.1016/j.bbrc.2012.02.068.
565 11. Nejati F, Junne S, Neubauer P. A Big World in Small Grain: A Review of Natural Milk Kefir
566 Starters. Microorganisms. 2020;8(2). doi: 10.3390/microorganisms8020192.
567 12. Klijn N, Weerkamp AH, de Vos WM. Genetic marking of *Lactococcus lactis* shows its survival in the
568 human gastrointestinal tract. Appl Environ Microbiol. 1995;61(7):2771-2774. doi: 10.1128/aem.61.7.2771-
569 2774.1995.
570 13. Kimoto-Nira H. New lactic acid bacteria for skin health via oral intake of heat-killed or live cells.
571 Anim Sci J. 2018;89(6):835-842. doi: 10.1111/asj.13017.
572 14. Sugimura T, Jounai K, Ohshio K, Tanaka T, Suwa M, Fujiwara D. Immunomodulatory effect of
573 *Lactococcus lactis* JCM5805 on human plasmacytoid dendritic cells. Clin Immunol. 2013;149(3):509-518. doi:
574 10.1016/j.clim.2013.10.007.

575 15. Nomura M, Kobayashi M, Narita T, Kimoto-Nira H, Okamoto T. Phenotypic and molecular
576 characterization of *Lactococcus lactis* from milk and plants. J Appl Microbiol. 2006;101(2):396-405. doi:
577 10.1111/j.1365-2672.2006.02949.x.
578 16. Fallico V, McAuliffe O, Fitzgerald GF, Ross RP. Plasmids of raw milk cheese isolate Lactococcus
579 lactis subsp. lactis biovar diacetylactis DPC3901 suggest a plant-based origin for the strain. Appl Environ
580 Microbiol. 2011;77(18):6451-6462. doi: 10.1128/AEM.00661-11.
581 17. Kimoto H, Mizumachi K, Okamoto T, Kurisaki J. New *Lactococcus* strain with immunomodulatory
582 activity: enhancement of Th1-type immune response. Microbiol Immunol. 2004;48(2):75-82. doi:
583 10.1111/j.1348-0421.2004.tb03490.x.
584 18. Suzuki C, Kimoto-Nira H, Kobayashi M, Nomura M, Sasaki K, Mizumachi K. Immunomodulatory
585 and cytotoxic effects of various *Lactococcus* strains on the murine macrophage cell line J774.1. Int J Food
586 Microbiol. 2008;123(1-2):159-165. doi: 10.1016/j.ijfoodmicro.2007.12.022.
587 19. Nakano K, Minami M, Shinzato M, Shimoji M, Ashimine N, Shiroma A, et al. Complete genome
588 sequence of *Lactococcus lactis* subsp. lactis G50 with immunostimulating activity, isolated from Napier grass.
589 Genome Announc. 2018;6(8). doi: 10.1128/genomeA.00069-18.
590 20. Tanaka M, Odani T, Yuuki T, Ohtake Y, Shimma Y-I, Yoko-O T, et al. Yeast strain releasing
591 mannan protein and method of producing mannan protein WO2006025295A1 2005.
592 21. Nomura M, Kobayashi M, Okamoto T. Rapid PCR-based method which can determine both
593 phenotype and genotype of Lactococcus lactis subspecies. Appl Environ Microbiol. 2002;68(5):2209-2213. doi:
594 10.1128/AEM.68.5.2209-2213.2002.
595 22. Nomura M, Kimoto H, Someya Y, Suzuki I. Novel characteristic for distinguishing Lactococcus
596 lactis subsp. lactis from subsp. cremoris. Int J Syst Bacteriol. 1999;49 Pt 1:163-166. doi: 10.1099/00207713-49-
597 1-163.
598 23. Kimoto H, Nomura M, Suzuki I. Growth energetics of *Lactococcus lactis* subsp. *lactis* biovar
599 diacetylactis in cometabolism of citrate and glucose. International Dairy Journal. 1999;9(12):857-863.
600 24. Meyrand M, Guillot A, Goin M, Furlan S, Armalyte J, Kulakauskas S, et al. Surface proteome
601 analysis of a natural isolate of *Lactococcus lactis* reveals the presence of pili able to bind human intestinal
602 epithelial cells. Mol Cell Proteomics. 2013;12(12):3935-3947. doi: 10.1074/mcp.M113.029066.
603 25. Holm L, Rosenstrom P. Dali server: conservation mapping in 3D. Nucleic Acids Res. 2010;38(Web
604 Server issue):W545-549. doi: 10.1093/nar/gkq366.
605 26. Kabsch W. XDS. Acta Crystallogr D Biol Crystallogr. 2010;66(Pt 2):125-132. doi:
606 10.1107/S0907444909047337.
607 27. Evans P. Scaling and assessment of data quality. Acta Crystallogr D Biol Crystallogr. 2006;62(Pt
608 1):72-82. doi: 10.1107/S0907444905036693.
609 28. Winn MD, Ballard CC, Cowtan KD, Dodson EJ, Emsley P, Evans PR, et al. Overview of the CCP4
610 suite and current developments. Acta Crystallogr D Biol Crystallogr. 2011;67(Pt 4):235-242. doi:
611 10.1107/S0907444910045749.
612 29. Vagin A, Teplyakov A. Molecular replacement with MOLREP. Acta Crystallogr D Biol Crystallogr.
613 2010;66(Pt 1):22-25. doi: 10.1107/S0907444909042589.

614 30. Yang YH, Jiang YL, Zhang J, Wang L, Bai XH, Zhang SJ, et al. Structural insights into SraP-
615 mediated *Staphylococcus aureus* adhesion to host cells. PLoS Pathog. 2014;10(6):e1004169. doi:
616 10.1371/journal.ppat.1004169.
617 31. Emsley P, Cowtan K. Coot: model-building tools for molecular graphics. Acta Crystallogr D Biol
618 Crystallogr. 2004;60(Pt 12 Pt 1):2126-2132. doi: 10.1107/S0907444904019158.
619 32. Murshudov GN, Skubak P, Lebedev AA, Pannu NS, Steiner RA, Nicholls RA, et al. REFMAC5 for
620 the refinement of macromolecular crystal structures. Acta Crystallogr D Biol Crystallogr. 2011;67(Pt 4):355-
621 367. doi: 10.1107/S0907444911001314.
622 33. Chen VB, Arendall WB, 3rd, Headd JJ, Keedy DA, Immormino RM, Kapral GJ, et al. MolProbity:
623 all-atom structure validation for macromolecular crystallography. Acta Crystallogr D Biol Crystallogr.
624 2010;66(Pt 1):12-21. doi: 10.1107/S0907444909042073.
625 34. Dieye Y, Oxaran V, Ledue-Clier F, Alkhalaf W, Buist G, Juillard V, et al. Functionality of sortase A
626 in *Lactococcus lactis*. Appl Environ Microbiol. 2010;76(21):7332-7337. doi: 10.1128/AEM.00928-10.
627 35. Kinoshita H, Ohuchi S, Arakawa K, Watanabe M, Kitazawa H, Saito T. Isolation of lactic acid
628 bacteria bound to the porcine intestinal mucosa and an analysis of their moonlighting adhesins. Biosci
629 Microbiota Food Health. 2016;35(4):185-196. doi: 10.12938/bmfh.16-012.
630 36. Amblee V, Jeffery CJ. Physical features of intracellular proteins that moonlight on the cell surface.
631 PLoS One. 2015;10(6):e0130575. doi: 10.1371/journal.pone.0130575.
632 37. MacKenzie DA, Tailford LE, Hemmings AM, Juge N. Crystal structure of a mucus-binding protein
633 repeat reveals an unexpected functional immunoglobulin binding activity. J Biol Chem. 2009;284(47):32444-
634 32453. doi: 10.1074/jbc.M109.040907.
635 38. Suzuki C, Shimma YI. P-type ATPase spf1 mutants show a novel resistance mechanism for the killer
636 toxin SMKT. Mol Microbiol. 1999;32(4):813-823. doi: 10.1046/j.1365-2958.1999.01400.x.
637 39. Pretzer G, Snel J, Molenaar D, Wiersma A, Bron PA, Lambert J, et al. Biodiversity-based
638 identification and functional characterization of the mannose-specific adhesin of *Lactobacillus plantarum*. J
639 Bacteriol. 2005;187(17):6128-6136. doi: 10.1128/JB.187.17.6128-6136.2005.
640 40. von Ossowski I, Satokari R, Reunanen J, Lebeer S, De Keersmaecker SC, Vanderleyden J, et al.
641 Functional characterization of a mucus-specific LPXTG surface adhesin from probiotic *Lactobacillus*
642 *rhamnosus* GG. Appl Environ Microbiol. 2011;77(13):4465-4472. doi: 10.1128/AEM.02497-10.
643 41. Camacho C, Coulouris G, Avagyan V, Ma N, Papadopoulos J, Bealer K, et al. BLAST+: architecture
644 and applications. BMC Bioinformatics. 2009;10:421. doi: 10.1186/1471-2105-10-421.
645 42. Yanagida F, Chen YS, Shinohara T. Searching for bacteriocin-producing lactic acid bacteria in soil. J
646 Gen Appl Microbiol. 2006;52(1):21-28. doi: 10.2323/jgam.52.21.
647 43. Siezen RJ, Starrenburg MJ, Boekhorst J, Renckens B, Molenaar D, van Hylckama Vlieg JE. Genome-
648 scale genotype-phenotype matching of two *Lactococcus lactis* isolates from plants identifies mechanisms of
649 adaptation to the plant niche. Appl Environ Microbiol. 2008;74(2):424-436. doi: 10.1128/AEM.01850-07.
650
651
652

653 # Supporting information

654 **S1_raw_Fig 1 image.** Two gels loaded with the same samples, one for CBB staining and one
655 for western blotting, were simultaneously subjected to SDS-PAGE. Proteins were visualized
656 by CBB staining (Left panel, Fig 1B) or western blotting visualizing by exposure with ECL
657 regent (Right panel, Fig 1A). The middle panel is the PVDF membrane after exposure with
658 ECL, visualizing the protein on which the ECL reagent bound.

659

660 **7YL4_D_1300030883_val-report-full_P1**. A PDB Summary Validation Report for 7YL4,
661 the ligand-free structure of $YwfG_{28–511}$.

662 **7YL5_D_1300030884_val-report-full_P1**. A PDB Summary Validation Report for 7YL5,
663 the D-mannose complex structure of $YwfG_{28–511}$.

664 **7YL6_D_1300030939_val-report-full_P1**. A PDB Summary Validation Report for 7YL6,
665 the α 1,2-mannobiose complex structure of $YwfG_{28–511}$.

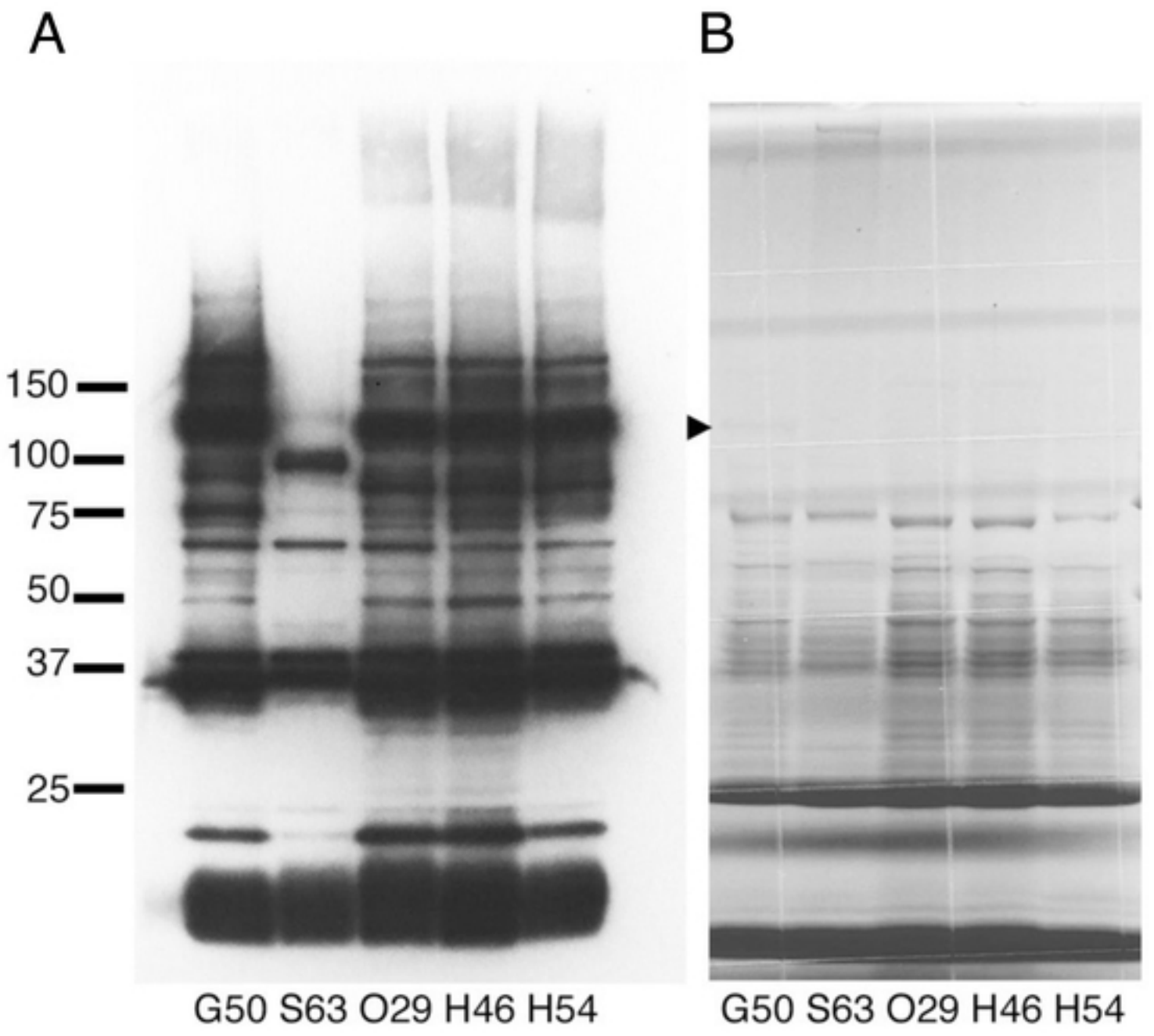

Fig 1

MNKKSSALLTMGTLTLLAGGGVVLTNLPDSFKIQRVYAATSRDITVYPKDFLTYFQRNGS 60

AAGFDYDLATYTQTLTPNKASQAGNVTLKTKVDMSQNFTFTGKINLGDKAQNAGGADGVG 120

FLFHPGDTNVVGAPGGAAGIGGVNGAFGFKLDTYYNGVGENSFTPDPSNFKGKPFGAFVD 180

GLNGQAKTIASSAQSISEPSNNNFVDFTMSYNGATKVMSVTYGGQTWTQDVSSFVGTNQA 240

MSFSIAASTGAFMNLQQLRNVNFTYTVAQGTVIANYVDEQGNTIAQQETTSGDIDTPYVT 300

SQKTIPGYTFKASNGAATSGNYAANDQTVNYVYTRNQGSIDVTYIDQTTGQTLSKKDLSG 360

GTGDSSNYTTADTIKSYTDAGYELVSDNYPSGGTVFTDTAQHYVVNLKQKLVVSSEQKQV 420

NETIQYVYEDGSKAADDYNAPPLNFTRSVTTNQVTGEKTYGDWQAQNGDSFGEVVSPTIK 480

GETADQLKIDAISGITANSADIQKKVVYKRNQGTIDVTYIDETTGQVLTKKDLSGGTDDP 540

SNYTTADDIKSYTAKGYELVSDDYPSGGTVFTDEPQHYVVKLKHGLTESTDKKAVNQVIH 600

YVYEGGGEAATDHNATVDFSRTITTDRVTNDKTYGDWTADNGDSFASVTSPVIDGYTADQ 660

LKVSEMTGITADTEDISVTVTYTRNQGTIDITYIDQTTGQTLSEKDLSGGTGDDSGYTTA 720

DTIKSYTDKGYELVSNDYPEDGTKFADDPQHYIVRLKHGLTEVTENKTVNQVIHYVYEGG 780

GEAATDHNATVVFSQTITTDKVTGEKTYSDWTADNGDSFASVTSPVIDGYTADQLKVSEM 840

TGITVDTEDISVTVTYTRNQGTIDVTYIDETTGKILTTKDLSGGTGDDSGYTTADTIKSY 900

TDKGYELVSNDYPEDGTKFADDPQHYIVRLKHGTVVETENKSVNEVIHYVYDNGDKAADN 960

YKATIVFSRTITTDKVTGEKTYSDWTADNGGRFAAVLSPIIKDYIASQLKIDEMTGITVD 1020

TADIERIVVYHKVPAGIIVPPVHPDKPSQPSNNQSKTPTAKAVKDSKPTDVLPSTGDSQK 1080

SQIVLTLLGIMAVIISPLALLLRRRKQ 1107

Fig 2

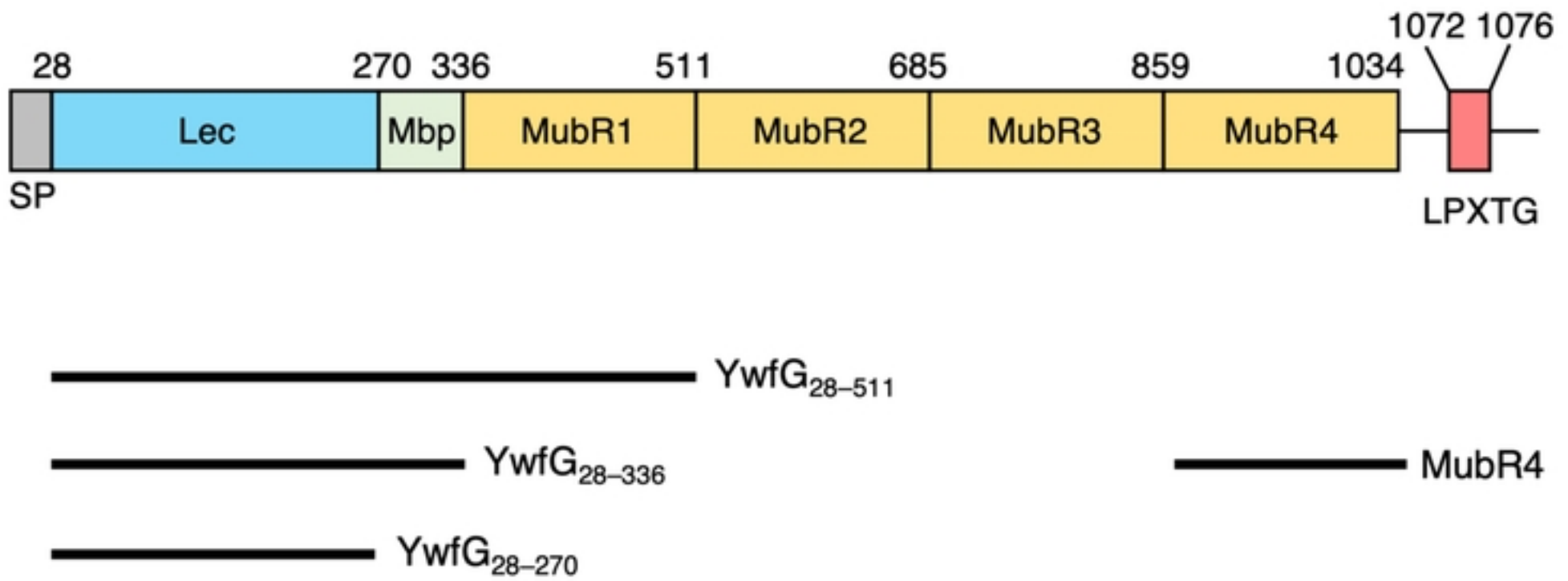
28
270
336
511
685
859
1034
1072
1076
Lec
Mbp
MubR1
MubR2
MubR3
MubR4
SP
LPXTG
YwfG28–511
YwfG28–336
YwfG28–270
MubR4

Fig 3

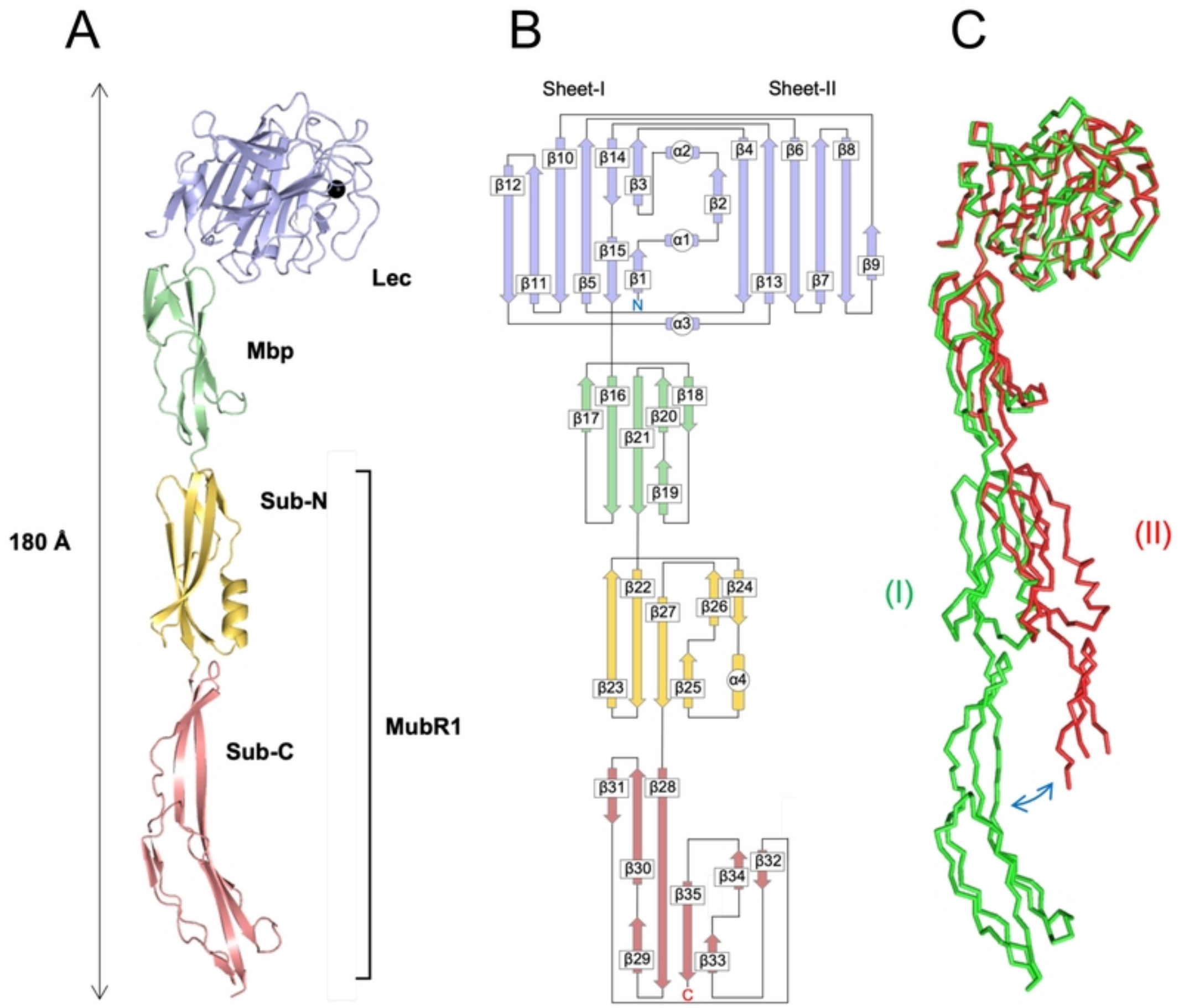
A
B
C
Lec
Mbp
Sub-N
Sub-C
180 Å
MubR1
Sheet-I
Sheet-II
β1
β2
β3
β4
β5
β6
β7
β8
β9
β10
β11
β12
β13
β14
β15
β16
β17
β18
β19
β20
β21
β22
β23
β24
β25
β26
β27
β28
β29
β30
β31
β32
β33
β34
β35
α1
α2
α3
α4
N
C
(I)
(II)

Fig 4

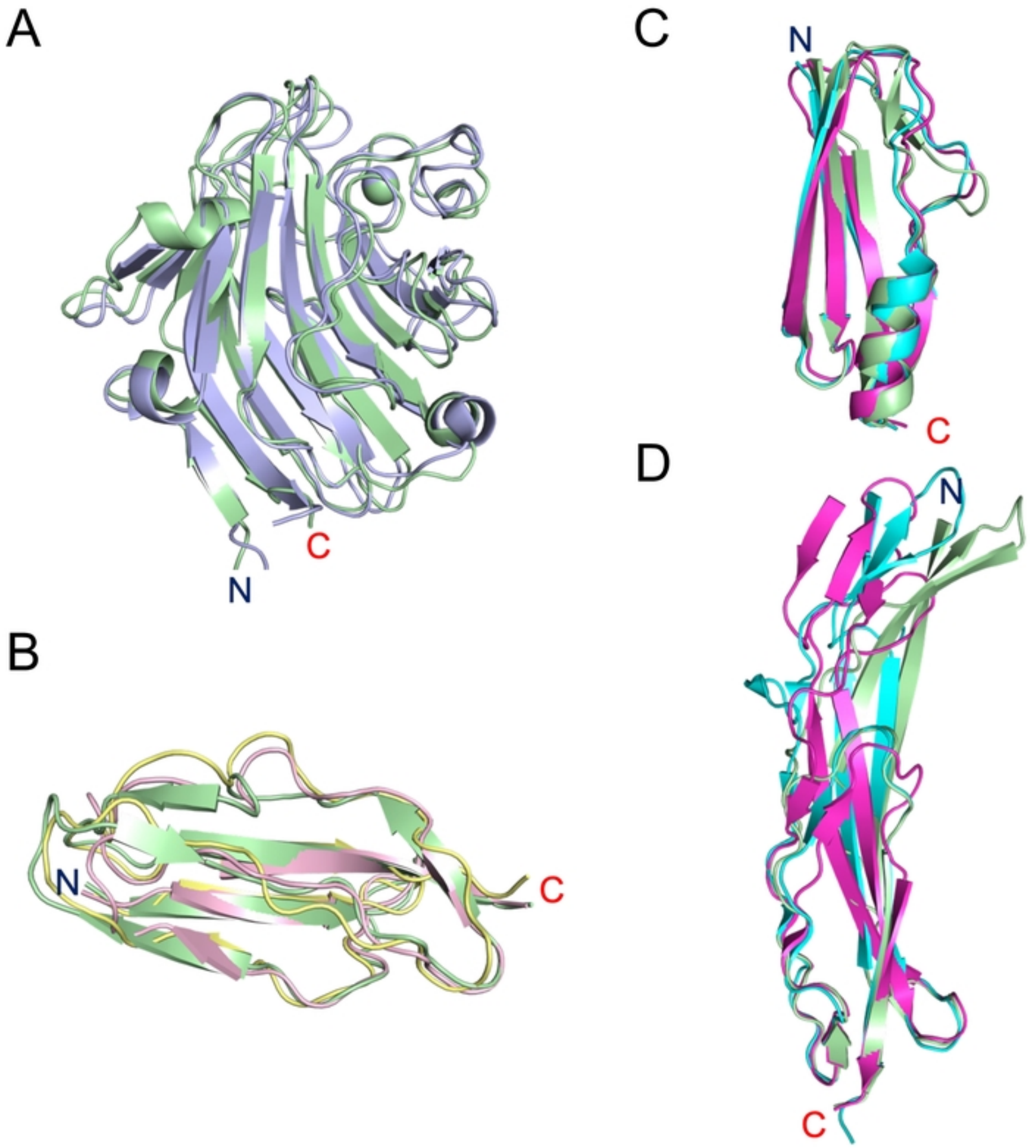

Fig 5

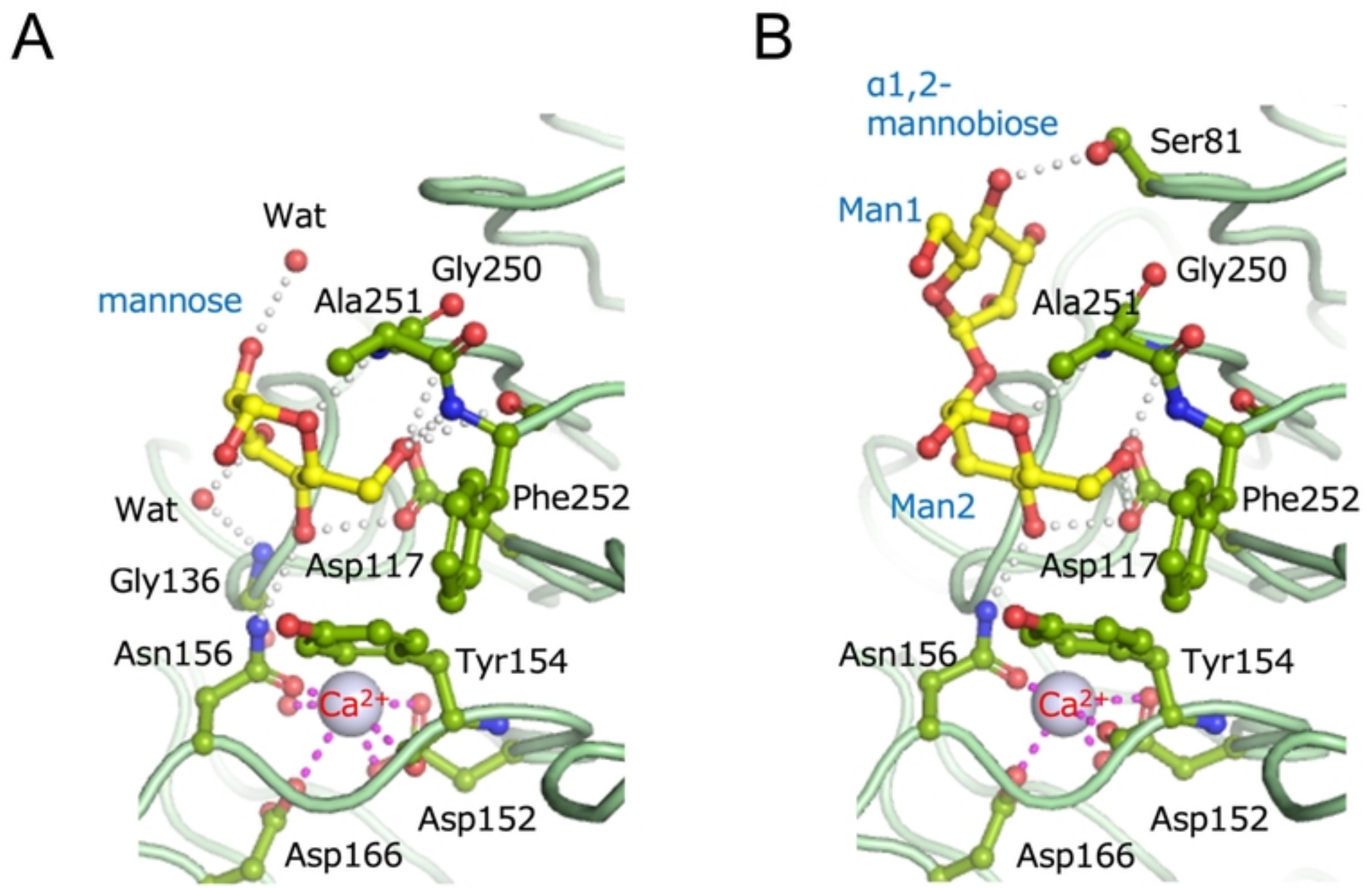
A
Wat
mannose
Gly250
Ala251
Wat
Phe252
Gly136
Asp117
Asn156
Tyr154
Ca2+
Asp152
Asp166
B
α1,2-
mannobiose
Ser81
Man1
Gly250
Ala251
Man2
Phe252
Asp117
Asn156
Tyr154
Ca2+
Asp152
Asp166

Fig 6

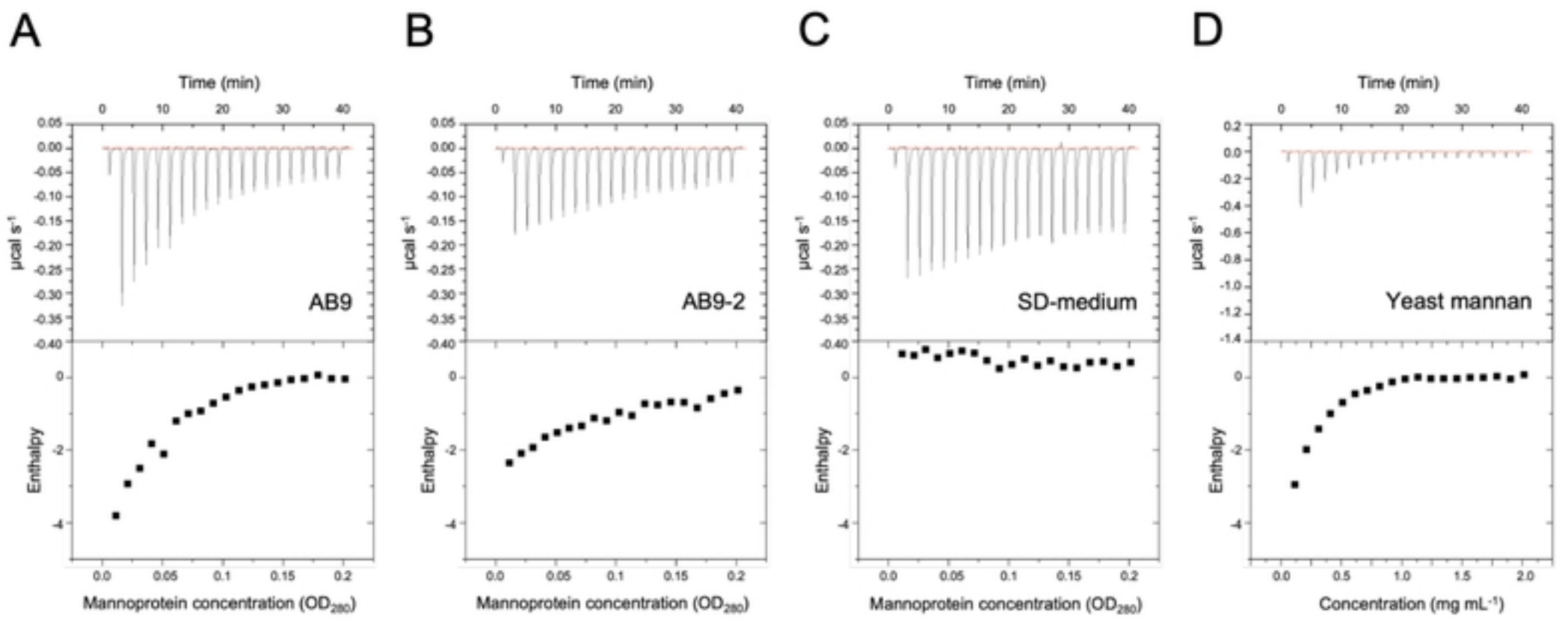
A
B
C
D
Time (min)
μcal s-1
AB9
AB9-2
SD-medium
Yeast mannan
Enthalpy
Mannoprotein concentration (OD280)
Concentration (mg mL-1)

Fig 7

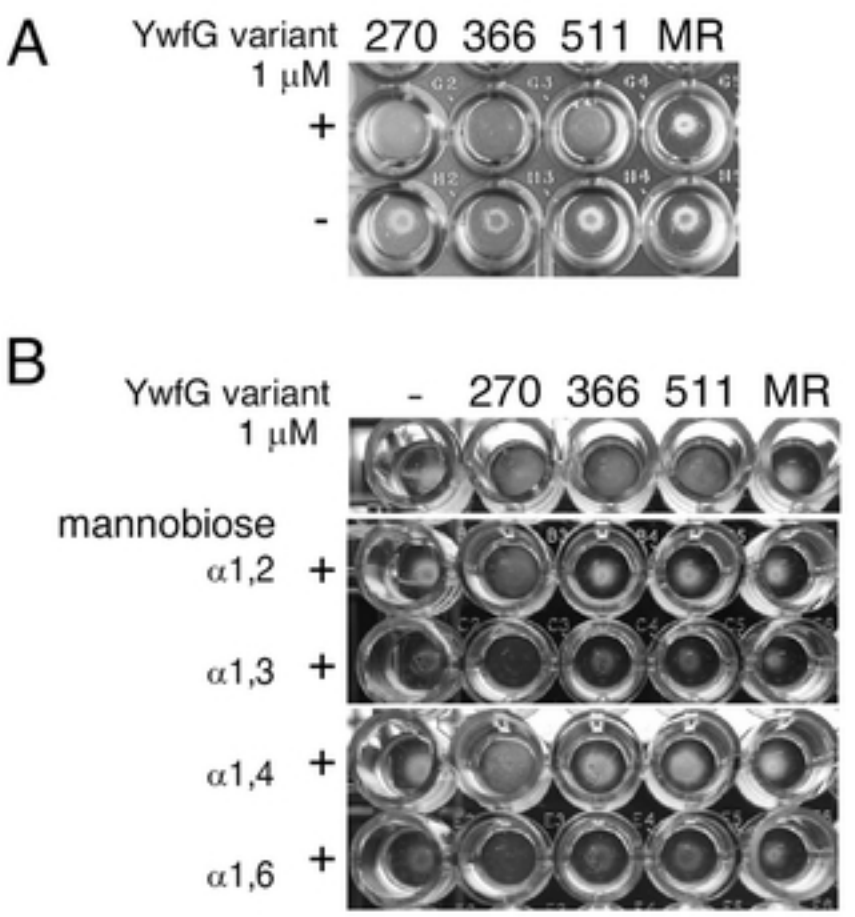
A
YwfG variant
270
366
511
MR
1 μM
+
-
B
YwfG variant
-
270
366
511
MR
1 μM
mannobiose
α1,2 +
α1,3 +
α1,4 +
α1,6 +

Fig 8

Western blotting (Figure 1A)

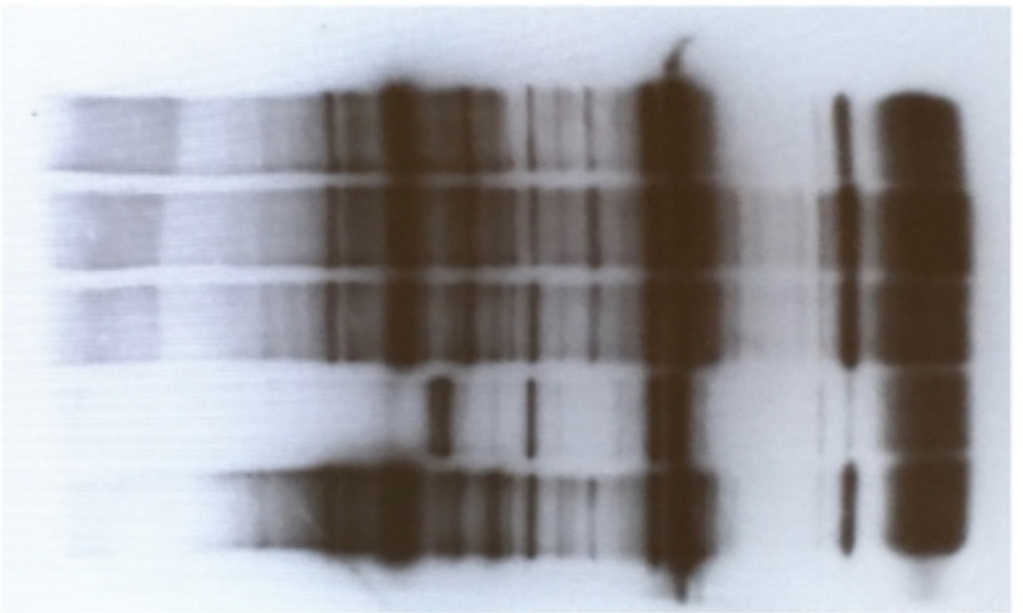

Blot membrane after exposure

CBB staining (Figure 1B)

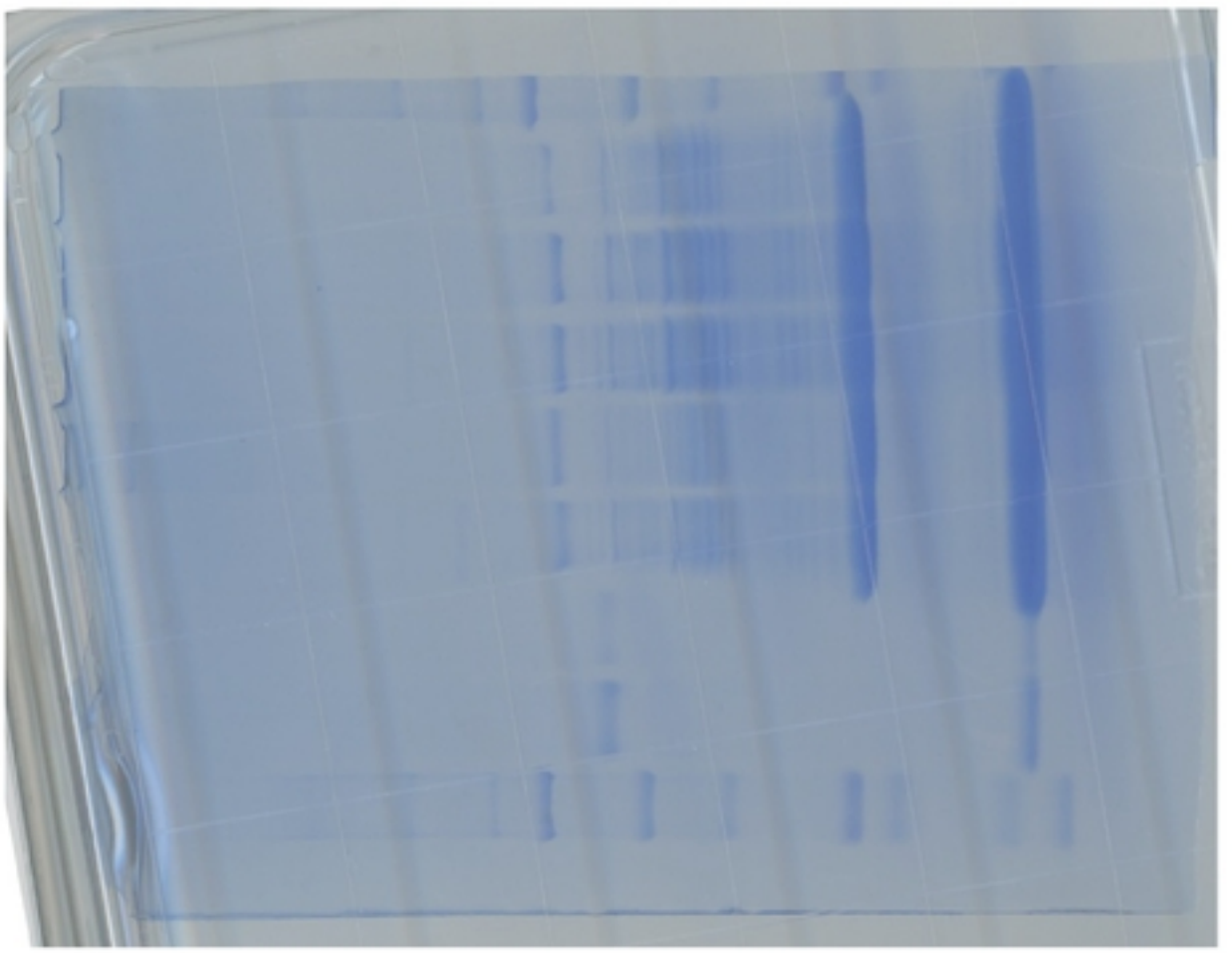

S1_raw_Fig 1 image